Monatshefte für Chemie 132, 1363–1386 (2001)

Monatshefte für Chemie
Chemical Monthly

Printed in Austria

Invited Review

Prediction of Electrolyte Solubilities from Minimal Thermodynamic Information

Erich Königsberger[*]

Department of Chemistry, School of Mathematical and Physical Sciences, Murdoch University, Murdoch WA 6150, Australia

Summary. A method is proposed that permits the proper extrapolation of thermodynamic quantities represented by the *Pitzer* equations from 25°C to other temperatures. The new method, which assumes temperature independent heat capacities, was tested for the NaCl–H_2O system and found very satisfactory. A new evaluation of the Na_2CO_3–H_2O system according to the CALPHAD method is presented, and solubilities for the quaternary Na_2CO_3–NaCl–NaOH–H_2O and its ternary subsystems are predicted. Limitations of (*i*) these predictions and of (*ii*) the *Pitzer* model regarding extrapolations to high molalities are discussed.

Keywords. Solubility; Phase diagram; *Pitzer* model, SIT; Enthalpy; Heat capacity; Sodium chloride; Sodium carbonate.

Introduction

It is often believed that macroscopically observable properties of electrolyte systems, like thermodynamic quantities or solubilities, can be derived from solid-solute-solvent interactions once computers have become powerful enough to solve complicated equations in order to calculate 'everything' from first principles. In contrast, holism claims that completely new qualities emerge in macroscopic systems, and simple reductionism is a fundamentally wrong concept because microscopic and macroscopic properties are complementary to each other in the sense of *Niels Bohr*'s famous concept [1]. In fact, all molecular-level theories, but also empirical models, have failed so far to predict, for instance, solubilities of ionic solids over wide ranges of temperature, pressure, and composition in sufficient accuracy for industrial, geochemical, or environmental applications.

Nevertheless, in recent years the *semi*-empirical ion-interaction model developed by *Pitzer* [2] has been successfully applied to solubility calculations in multicomponent electrolyte solutions at ambient [3, 4] and other temperatures

---

[*] On leave from Institut für Physikalische Chemie, Montanuniversität Leoben, A-8700 Leoben, Austria. E-mail: koenigsb@chem.murdoch.edu.au

ranging from $T = -60°\text{C}$ to $T = 250°\text{C}$ [5–13]. Whereas database development by geochemical groups [5, 8–13] usually involves fitting of solubility products to experimental solubility data as a function of temperature, *Pabalan* and *Pitzer* [6, 7] employed a procedure similar to what has been known for a long time as the CALPHAD method.

Kaufman and others originally developed the CALPHAD (CALculation of PHAse Diagrams) method [14] to perform equilibrium calculations on heterogeneous, high-temperature systems involving phases like alloys, slags, oxides, or silicates. Using so-called optimization programs, various kinds of experimental information (phase equilibria, activities, enthalpies, heat capacities, densities, *etc.*) are employed to evaluate *Gibbs* energies of the individual phases as functions of temperature, pressure, and composition. Thereby, parameters of appropriate *semi*-empirical models are adjusted that describe the excess properties of the various non-ideal phases as closely as possible. Since quaternary interactions are normally negligible, the optimizations are performed on binary and ternary systems in order to correlate their thermodynamic properties, and the model equations are then used to predict the thermodynamic properties of multicomponent systems.

The present author has employed the CALPHAD method for the assessment of electrolyte systems involving highly or sparingly soluble solid phases [15–20]. Carefully evaluated thermodynamic data have been used for the calculation of solubility equilibria with applications to geochemistry [16–26] and to the simulation of industrial processes [27]. In this communication, an attempt is made to predict solubilities of highly soluble ionic solids in the temperature range from 0 to 100°C using only limited experimental information valid for 25°C as model input. Therefore, proper extrapolation of solution thermodynamic properties to other temperatures is crucial and will be examined in detail. The *Pitzer* model [2] will be mainly used, but some remarks on the *Brønsted-Guggenheim-Scatchard* specific ion-interaction theory (SIT) proposed by *Grenthe et al.* [28] will be given as well. Solubility predictions for the $NaCl–NaOH–Na_2CO_3–H_2O$ system and its subsystems will be presented and their limitations will be discussed.

The *Pitzer* Model: A Story of Success with Limitations

In 1973, *Pitzer* [29] developed a set of equations that can accurately represent the excess properties of electrolyte solutions as a function of composition, temperature, and pressure. The total excess *Gibbs* energy, G^E, of a binary solution is given by

$$G^{\mathrm{E}} = w_{\mathrm{w}} \nu m R T (1 - \phi + \ln\gamma_{\pm}), \tag{1}$$

where R and T have their usual meaning, w_w is the mass of the solvent, $\nu = \nu_M + \nu_X$ (ν_M, ν_X: stoichiometric coefficients of cations and anions, respectively), m is the molality, ϕ is the osmotic coefficient of the solvent, and $\gamma_{\pm}$ is the mean activity coefficient of the solute. In the *Pitzer* model, G^E contains a *Debye-Hückel* term, a representation of the ionic strength dependence of the second virial coefficient B_{MX}, and a third viral coefficient C_{MX} that is independent of ionic strength:

$$G^{\mathrm{E}}/(w_{\mathrm{w}} R T) = -A_{\phi}(4 I b^{-1}) \ln(1 + b I^{1/2}) + 2\nu_{\mathrm{M}}\nu_{\mathrm{X}}(m^2 B_{\mathrm{MX}} + m^3 \nu_{\mathrm{M}} z_{\mathrm{M}} C_{\mathrm{MX}}) \tag{2}$$

$$B_{\mathrm{MX}} = \beta^{(0)}_{\mathrm{MX}} + 2\beta^{(1)}_{\mathrm{MX}}(1 - (1 + \alpha_1 I^{1/2})\exp(-\alpha_1 I^{1/2}))(\alpha_1^2 I)^{-1}$$
$$+ 2\beta^{(2)}_{\mathrm{MX}}(1 - (1 + \alpha_2 I^{1/2})\exp(-\alpha_2 I^{1/2}))(\alpha_2^2 I)^{-1} \quad (3)$$

In Eqs. (2) and (3), I is the ionic strength on molality basis, A_ϕ is the *Debye-Hückel* coefficient for the osmotic function (at 25°C, $A_\phi = 0.3915\,\mathrm{kg}^{1/2}\cdot\mathrm{mol}^{-1/2}$), and z_i are the charges of the ions i. The constant b equals 1.2 for all solutes, $\alpha_1 = 2$ and $\alpha_2 = 0$ (*i.e.* $\beta^{(2)}_{\mathrm{MX}}$ is not required) unless both ions have a charge greater than or equal to 2, in which case $\alpha_1 = 1.4$ and $\alpha_2 = 12$. For 3–2 and 4–2 electrolytes, $\alpha_1 = 2$ and $\alpha_2 = 50$ have been used [2]. It should be noted that b, α_1, and α_2 are assumed to be temperature independent. Thus, at fixed pressure and temperature, G^E is expressed in terms of up to four adjustable parameters $\beta^{(0)}_{\mathrm{MX}}$, $\beta^{(1)}_{\mathrm{MX}}$, $\beta^{(2)}_{\mathrm{MX}}$, and C_{MX} per electrolyte, which are generally fitted to osmotic and/or activity coefficient data. Values of $\beta^{(2)}_{\mathrm{MX}}$ are relatively large and negative for solutes which are significantly ion-paired. However, if the value of the ion-association constant exceeds some critical value, the resulting complexes are usually taken into account as individual species [4]. Instead of C_{MX}, the quantity that is often tabulated is the parameter occurring in the expression for the osmotic coefficient, C^ϕ_{MX}, which is defined as

$$C_{\mathrm{MX}} = C^\phi_{\mathrm{MX}}(2|z_\mathrm{M} z_\mathrm{X}|^{1/2})^{-1} \quad (4)$$

Equations for ϕ and $\ln\gamma_\pm$, which are related to the partial molar excess *Gibbs* energies of solvent and solute, are obtained by appropriate differentiation [2]. *Pitzer* [2] also presents general equations for G^E, ϕ, and $\ln\gamma_\pm$ that are valid for multicomponent solutions. For the latter, higher-order electrostatic terms, ${}^\mathrm{E}\theta(I)$, which arise from asymmetric mixing, *e.g.* between HCO_3^- and CO_3^{2-}, and are functions of the ionic strength, are usually taken into account. In addition, the parameters ${}^\mathrm{S}\theta_{\mathrm{M,M'}}$, ${}^\mathrm{S}\theta_{\mathrm{X,X'}}$, $\psi_{\mathrm{M,X,X'}}$, and $\psi_{\mathrm{M,M',X}}$ are used to describe specific interactions in ternary systems. *Pitzer* [2] presents a convenient method to calculate ${}^\mathrm{E}\theta(I)$, as well as extensive tables of interaction parameters.

Equations for apparent molar volumes, enthalpies, and heat capacities can be derived from the excess *Gibbs* energy by appropriate differentiation with respect to pressure or temperature. In this communication, the effect of temperature on G^E is of particular interest. Thus, the relative enthalpy, L, and the relative heat capacity, J, of the solution must be known, which are defined according to Eqs. (5) and (6).

$$L = H - H^\circ = -T^2(\partial(G^\mathrm{E}/T)/\partial T)_{P,m} \quad (5)$$

$$J = C_p - C_p^\circ = (\partial L/\partial T)_{P,m}$$
$$= -T^2(\partial^2(G^\mathrm{E}/T)/\partial T^2 + (2/T)(\partial(G^\mathrm{E}/T)/\partial T))_{P,m} \quad (6)$$

In Eqs. (5) and (6), the superscript ° denotes the total quantity of the components in their standard states. The apparent molar relative enthalpy, ${}^\phi L$, and the apparent molar heat capacity, ${}^\phi C_p$, are defined as

$${}^\phi L = L/n_2 \quad (7)$$

and

$${}^\phi C_p = (C_p - n_1 C^\circ_{p1})/n_2 = C^\circ_{p2} + (\partial{}^\phi L/\partial T)_{P,m}, \quad (8)$$

where C°_{p1} and C°_{p2} are the molar heat capacity of pure water and the partial molar heat capacity of the electrolyte at infinite dilution, respectively, and $n_2 = w_{\mathrm{w}} m$ is the amount of solute.

Taking the appropriate derivative of Eq. (2) as given by Eqs. (5) and (7) results in the expression for the relative apparent molar enthalpy.

$$^{\phi}L = v|z_{\mathrm{M}}z_{\mathrm{X}}|A_L(2b)^{-1}\ln(1+bI^{1/2}) - 2v_{\mathrm{M}}v_{\mathrm{X}}RT^2(mB^L_{\mathrm{MX}} + m^2 v_{\mathrm{M}}z_{\mathrm{M}}C^L_{\mathrm{MX}}) \tag{9}$$

$$B^L_{\mathrm{MX}} = (\partial B_{\mathrm{MX}}/\partial T)_{P,m} \tag{10}$$

$$\beta^{(\mathrm{i})L}_{\mathrm{MX}} = (\partial \beta^{(\mathrm{i})}_{\mathrm{MX}}/\partial T)_P \quad \text{for i} = 0,1,2 \tag{11}$$

$$C^L_{\mathrm{MX}} = (\partial C_{\mathrm{MX}}/\partial T)_P = (\partial C^{\phi}_{\mathrm{MX}}/\partial T)_P\,(2|z_{\mathrm{M}}z_{\mathrm{X}}|^{1/2})^{-1} \tag{12}$$

In Eq. (9), the *Debye-Hückel* coefficient for enthalpy is defined by

$$A_L = 4RT^2(\partial A_{\phi}/\partial T)_P \tag{13}$$

and has the value $A_L/RT = 0.801\,\mathrm{kg}^{1/2}\cdot\mathrm{mol}^{-1/2}$ at 25°C. The apparent molar heat capacity is given by

$$\begin{aligned} ^{\phi}C_p = C^{\circ}_{p2} &+ v|z_{\mathrm{M}}z_{\mathrm{X}}|A_J(2b)^{-1}\ln(1+bI^{1/2}) \\ &- 2v_{\mathrm{M}}v_{\mathrm{X}}RT^2(mB^J_{\mathrm{MX}} + m^2 v_{\mathrm{M}}z_{\mathrm{M}}C^J_{\mathrm{MX}}) \end{aligned} \tag{14}$$

$$B^J_{\mathrm{MX}} = (\partial^2 B_{\mathrm{MX}}/\partial T^2)_{P,m} + (2/T)(\partial B_{\mathrm{MX}}/\partial T)_{P,m} \tag{15}$$

$$\beta^{(\mathrm{i})J}_{\mathrm{MX}} = (\partial^2 \beta^{(\mathrm{i})}_{\mathrm{MX}}/\partial T^2)_P + (2/T)(\partial \beta^{(\mathrm{i})}_{\mathrm{MX}}/\partial T)_P \quad \text{for i} = 0,1,2 \tag{16}$$

$$\begin{aligned} C^J_{\mathrm{MX}} &= (\partial^2 C_{\mathrm{MX}}/\partial T^2)_P + (2/T)(\partial C_{\mathrm{MX}}/\partial T)_P \\ &= ((\partial^2 C^{\phi}_{\mathrm{MX}}/\partial T^2)_P + (2/T)(\partial C^{\phi}_{\mathrm{MX}}/\partial T)_P)(2|z_{\mathrm{M}}z_{\mathrm{X}}|^{1/2})^{-1} \end{aligned} \tag{17}$$

In Eq. (14), the *Debye-Hückel* coefficient for heat capacity is defined by

$$A_J = (\partial A_L/\partial T)_P \tag{18}$$

and has the value $A_J/R = 3.94\,\mathrm{kg}^{1/2}\cdot\mathrm{mol}^{-1/2}$ at 25°C.

The unchallenged strength of the *Pitzer* model rests in its capability to correlate and reproduce, within the experimental uncertainty of high-precision measurements, the thermodynamic properties of electrolyte solutions over wide ranges of temperatures, pressures, and concentrations up to saturation. This has been convincingly demonstrated for osmotic coefficients, enthalpies of dilution, heat capacities, and molar volumes measured with unsurpassed precision and accuracy at Oak Ridge National Laboratory (ORNL) [30]. However, it is a major limitation of the *Pitzer* model that extrapolation to molalities exceeding the range covered during parametrization is generally poor. The $ZnSO_4$–H_2O system [15] provides a striking example. When the relative apparent molar enthalpy of $ZnSO_4(aq)$ is modelled with parameters reported by *Silvester* and *Pitzer* [31] to be valid up to $1\,\mathrm{mol}\cdot\mathrm{kg}^{-1}$, wrong signs of the temperature coefficients of zinc sulfate heptahydrate and hexahydrate solubilities are predicted. This results from a completely wrong extrapolation of $^{\phi}L$ to saturation ($3.6\,\mathrm{mol}\cdot\mathrm{kg}^{-1}$). After adjusting the enthalpy parameters with respect to experimental data measured up to saturation, very good solubility predictions could be made for temperatures ranging from

10 to 70°C [15]. Other examples of wrong extrapolations will be discussed below.

To correlate high-precision experimental data over wide ranges of temperature, pressure, and composition, various modifications or extensions of the classical *Pitzer* equations have been proposed:

(*i*) To improve the fit, researchers have frequently changed the numerical value of α_1 (see *e.g.* Refs. [32–34]) or even used different α_1 values for the various components of a mixture [34]. Adjustable α_2 values and $\beta_{\mathrm{MX}}^{(2)}$ parameters have also been employed for 1–1 electrolytes to account for ion association at the highest temperatures [32, 35]. Moreover, there is some confusion regarding the definition of the C^L parameters (sometimes denoted as C') owing to different forms of the equation used for ${}^{\phi}L$ [32, 35, 36].

(*ii*) To correlate electrolyte properties to very high ionic strengths (*e.g.* $33\,\mathrm{mol}\cdot\mathrm{kg}^{-1}$ for $CaCl_2$), the *Pitzer* equations have been extended using virial coefficients up to the sixth order [37]. *Archer* introduced an ionic-strength term at the third level for NaBr [38] and NaCl [39], and his equations have been generalized by *Clegg*, *Rard*, and *Pitzer* [40] to electrolyte mixtures. *Pitzer et al.* [41] recently presented a general form of equations that retains the expressions of the second virial level for all higher coefficients. Although similar to one another, these approaches are not completely compatible. Thus, either different equations have to be used or the parameters have to be refitted to the most general form given in Ref. [41].

(*iii*) The use of different equations for the dielectric constant of water and different equations of state of water resulted in various compilations of the *Debye-Hückel* limiting law slopes A_ϕ, A_L, and A_J as well as those for apparent molar volumes and compressibilities [42–44]. Nowadays, the *Bradley-Pitzer* equations [43] are most frequently used for the calculation of the *Debye-Hückel* slopes. Researchers of ORNL found in their recent study [45] that at temperatures from $T = 25$°C to 250°C and pressures $P \leq 400$ bar the values taken from Ref. [43] are essentially identical to those given more recently by *Archer* and *Wang* [44].

Therefore, care must be taken when combining *Pitzer* coefficients from different sources, as the parameters are generally not compatible with any single form of the *Pitzer* equations.

Making Predictions Using Limited Information

For a small number of about two dozen electrolytes, *Pitzer* parameters are known over a wide range of temperatures and are, for instance, fitted to equations of the form [46]

$$X(T) = w_1 + w_2(T/\mathrm{K})^{-1} + w_3 \ln(T/\mathrm{K}) + w_4(T/\mathrm{K}) + w_5(T/\mathrm{K})^2 + w_6(680 - T/\mathrm{K})^{-1} + w_7(T/\mathrm{K} - 227)^{-1} \qquad (19)$$

For the vast majority of electrolytes, however, *Pitzer* parameters for osmotic and activity coefficients [2, 47, 48], apparent molar enthalpies [2, 31], and heat capacities [49, 50] are only available at 25°C. Nonetheless, there is an urgent need in many geochemical, environmental, and industrial applications to estimate activity coefficients in mixed electrolyte solutions in the temperature range from 0 to 100°C.

For carbonate systems, *Monnin* and *Schott* [5] as well as *Pitzer* and associates [51, 52] have used the following power series expression

$$X(T) = X_0 + a(T - T_0) + (1/2)b(T - T_0)^2 \tag{20}$$

to estimate activity and osmotic coefficients from 0 to 50°C. In Eq. (20), $X(T)$ denotes the interaction parameter at temperature T, X_0 is its value at $T_0 = 298.15\,\mathrm{K}$, $a = (\partial X/\partial T)_P$, and $b = (\partial^2 X/\partial T^2)_P$ at $T = T_0$. The constants a and b can be expressed in terms of enthalpy and heat capacity parameter values valid at T_0, which are denoted as X^L and X^J, respectively. Using the definitions given in Eqs. (11), (12), (16), and (17), $a = X^L$ and $b = X^J - 2X^L/T_0$ are found.

Criss and *Millero* [49] suggested equations of the form

$$X(T) = X_0 + a(1/T - 1/T_0) + b(T^2 - T_0^2) \tag{21}$$

and claimed that reasonable estimates of activity coefficients are provided from 0 to 75°C and from 0 to $2\,\mathrm{mol \cdot kg^{-1}}$ in the ionic strength. In Eq. (21), $a = X^J T_0^3/3 - X^L T_0^2$ and $b = X^J/6$.

The new method proposed in this work (hereafter referred to as the present model) is based on temperature independent heat capacities.

$$X(T) = X_0 + a(1/T - 1/T_0) + b \ln(T/T_0). \tag{22}$$

In Eq. (22), $a = X^J T_0^3 - X^L T_0^2$ and $b = X^J T_0^2$. If there are no heat capacity parameters available, $X^J = 0$ and thus $a = -X^L T_0^2$ and $b = 0$. Quite frequently, only X_0 parameters have been reported and neither X^L nor X^J are available. Then, Eq. (22) would result in $X(T) = X_0$, *i.e.* the contribution to the excess *Gibbs* energy would be purely entropic. It is better, however, to assume that the contribution to the excess *Gibbs* energy is solely enthalpic. In this case, the convention used in the F*A*C*T database [53, 54] (see below) is employed, and $a = X_0 T_0$ is defined in a way that

$$X(T) = X_0 T_0/T \quad \text{only if } X^L = X^J = 0 \tag{23}$$

The applicability and limitations of Eqs. (20)–(23) will be investigated in the subsequent sections.

Solubility Calculations *via Gibbs* Energy Minimization

The widespread use and popularity of the CALPHAD method is based on the crucial role that the *Gibbs* energy plays in thermodynamic calculations. Not only

(*i*) all the other thermodynamic quantities can be derived by appropriate differentiation as indicated above, but also
(*ii*) the minimum of the *Gibbs* energy at constant temperature and pressure with respect to the composition of the various phases defines the thermodynamic equilibrium state of the heterogeneous system.

So-called *Gibbs* energy minimizers have been developed to perform these calculations reliably and, on modern computers, with sufficient speed even for multicomponent, multiphase systems. For each phase, the input data comprise parameters describing the temperature and pressure dependencies of (*i*) the standard *Gibbs* energies of all phase constituents and (*ii*) the excess *Gibbs* energies described by appropriate models. Among others, ChemSage [55] with its optimizer [15] and F*A*C*T (Facility for the Analysis of Chemical Thermodynamics) [53] are particularly useful for systems involving aqueous solutions. Both ChemSage and F*A*C*T feature the classical *Pitzer* model, in which the *Debye-Hückel* parameters are calculated according to *Bradley* and *Pitzer* [43]. There are two modifications of the model in which unsymmetrical, higher-order electrostatic mixing terms can be either taken into account or not. In ChemSage, the *Brønsted-Guggenheim-Scatchard* specific ion-interaction theory [28] and the *Helgeson-Kirkham-Flowers* model [56] are implemented as well. In the present work, all calculations and optimizations have been performed using ChemSage [15, 55].

Sodium Chloride

The NaCl–H_2O system is definitely the most thoroughly investigated binary electrolyte system and has therefore often served as a reference for testing thermodynamic models. In several reviews [39, 42, 46, 57], various modifications of the *Pitzer* equations have been employed to correlate the thermodynamic properties over the entire experimentally accessible temperature, pressure, and concentration ranges. *Archer*'s model [39] uses as many as 57 adjustable parameters, but it covers the most extended temperature and pressure ranges ($250 < T/\mathrm{K} < 600$, $P \leq 1000\,\mathrm{bar}$) of these studies.

As explained above, the present model uses the classical *Pitzer* equations with the 9 parameters given in Table 1. The interaction parameters valid at 25°C and the heat capacity parameters together with the partial molar heat capacities at infinite dilution of the ions were taken from *Pitzer* and *Mayorga* [47] and *Criss* and *Millero* [49], respectively, and used without modification. The enthalpy parameters of *Silvester* and *Pitzer* [31] do not reproduce experimental values very well, probably due to the use of an A_L value that is different from *Bradley* and *Pitzer*'s [43] definition. Thus, the enthalpy parameters were re-fitted to apparent molar relative enthalpies of NaCl at 25°C taken from *Parker* [58] and the NBS tables [59]. Since the temperature dependence of solubility depends on the partial molar enthalpy of NaCl at saturation [60], which in turn is related to the derivative of the apparent molar relative enthalpy with respect to molality, a ten times higher weight was put on the two data points close to saturation.

Standard thermodynamic quantities (Table 2) were taken from

(a) CODATA [61] and *Criss* and *Millero* [49] for the aqueous ions,
(b) the F*A*C*T thermodynamic database [53] for ice, water, and steam (the latter is modelled as non-ideal gas using a second virial coefficient that is calculated from critical data according to the *Tsonopoulos* correlation [64]), and
(c) *Archer*'s work for NaCl [62] and $\mathrm{NaCl \cdot 2H_2O}$ [39]; however, the standard enthalpies have been slightly adjusted (within the reported uncertainties) to reproduce the solubility at 25°C (in the case of NaCl) and the peritectic temperature (in the case of $\mathrm{NaCl \cdot 2H_2O}$).

Table 1. Binary *Pitzer* parameters for osmotic coefficients, apparent molar relative enthalpies, and apparent molar heat capacities, all valid at 25°C; parameters without superscript were determined in the present study

	NaCl	Na_2CO_3	$NaHCO_3$	NaOH	HCl
$\beta_{MX}^{(0)}$	0.0765[a]	0.0362[c]	0.028[c]	0.0864[a]	0.1775[a]
$\beta_{MX}^{(1)}$	0.2664[a]	1.51[c]	0.044[c]	0.253[a]	0.2945[a]
C_{MX}^{ϕ}	0.00127[a]	0.0052[c]		0.0044[a]	0.0008[a]
$10^3 \cdot \beta_{MX}^{(0)L}$	0.7293	2.127	1.00[c]	0.5307	−0.3081[d]
$10^3 \cdot \beta_{MX}^{(1)L}$	0.9031	5.059	1.10[c]	0.7495	0.1419[d]
$2 \cdot 10^3 \cdot \lvert z_M z_X \rvert^{1/2} C_{MX}^{L}$	−0.1066	−0.3765		−0.1355	−0.06213[d]
$10^5 \cdot \beta_{MX}^{(0)J}$	−1.53[b]	−3.019[c]	−1.929[c]	−1.41[b]	−0.304[b]
$10^5 \cdot \beta_{MX}^{(1)J}$	−0.0365[b]	−15.425[c]	−3.562[c]	−3.76[b]	0.678[b]
$2 \cdot 10^5 \cdot \lvert z_M z_X \rvert^{1/2} C_{MX}^{J}$	0.1824[b]	0.460		0.134[b]	0.00372[b]

[a] *Pitzer* and *Mayorga* [47]; [b] *Criss* and *Millero* [49]; [c] *Peiper* and *Pitzer* [51]; [d] *Silvester* and *Pitzer* [31]

Table 2. Standard thermodynamic quantities of phase constituents ($P^\circ = 1$ bar)

	$\Delta_f H_{298}^\circ / \mathrm{kJ \cdot mol^{-1}}$	$S_{298}^\circ / \mathrm{J \cdot K^{-1} \cdot mol^{-1}}$	$C_{p298}^\circ / \mathrm{J \cdot K^{-1} \cdot mol^{-1}}$
$H_2O(g)$	−241.834[a]	188.834[a]	33.59[a]
$H_2O(l)$	−285.83[b]	69.95[b]	75.38[a]
$H^+(aq)$	0	0	0
$Na^+(aq)$	−240.34[b]	58.45[b]	43.01[c]
$OH^-(aq)$	−230.015[b]	−10.90[b]	−140.80[c]
$Cl^-(aq)$	−167.08[b]	56.60[b]	−126.32[c]
$HCO_3^-(aq)$	−689.93[b]	98.4[b]	−54.23[d]
$CO_3^{2-}(aq)$	−675.23[b]	−50.0[b]	−314.5[d]
$CO_2(aq)$	−413.26[b]	119.36[b]	185.73[e]
$H_2O(s)$	−292.816[a]	44.529[a]	36.246[a,f]
$NaCl(s)$	−411.22[g]	71.97[h]	50.23[h]
$NaCl \cdot 2H_2O(s)$	−997.69[g]	162.51[i]	137.0[i]
$Na_2CO_3 \cdot 10H_2O(s)$	−4080.068[g]	560.98[g]	550.31[j]
$Na_2CO_3 \cdot 7H_2O(s)$	−3199.133[g]	423.20[g]	420[j]
$Na_2CO_3 \cdot H_2O(s)$	−1430.980[g]	164.66[g]	145.6[j]

[a] F*A*C*T database [53]; [b] CODATA key value [61]; [c] *Criss* and *Millero* [49]; [d] *Peiper* and *Pitzer* [51]; [e] *Königsberger et al.* [19]; [f] constant value at $T < 0$°C; [g] this work; [h] *Archer* [62]; [i] *Archer* [39]; [j] *Vanderzee* [63]

Figure 1 shows apparent molar heat capacities of NaCl(*aq*) at various temperatures. In the present model (Eq. (22)) the heat capacities are treated as temperature independent; the change of the calculated values with temperature is solely due the temperature dependence of the *Debye-Hückel* coefficient A_J (dash-dot line for 75°C). In the two other extrapolation methods, Eq. (21) and particularly Eq. (20), the heat capacity exhibits a much more pronounced temperature dependence (dashed and dotted lines, respectively, for 75°C).

In Fig. 2, relative apparent molar enthalpies are compared with values calculated according to the *Pitzer* and SIT models. The SIT model gives a reasonable fit at lower molalities, but if all data points are included, the 1-parameter SIT model

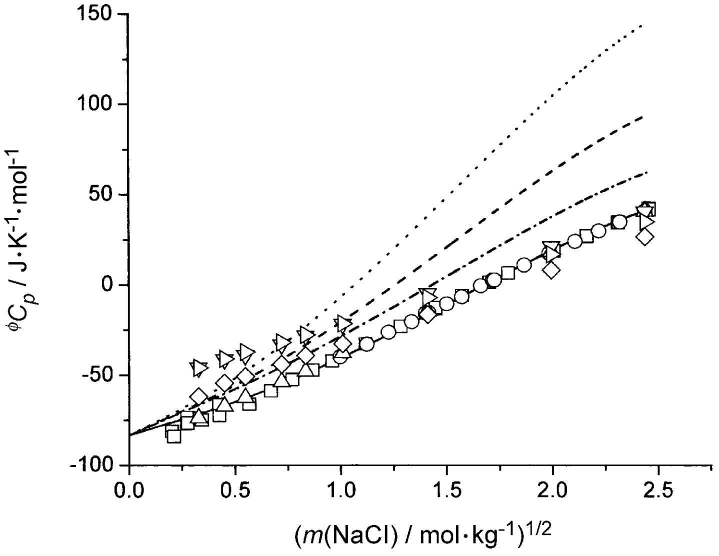

Fig. 1. Apparent molar heat capacities of NaCl(aq); experimental data at 25°C: squares [65], circles [66], up-triangles [67]; at 50°C: down triangles [67]; at 75°C: right-triangles [67]; at 100°C: diamonds [67]; calculated values at 25°C: solid line, present model; at 75°C: dash-dot line, present model; dashed line, according to Eq. (21); dotted line, according to Eq. (20)

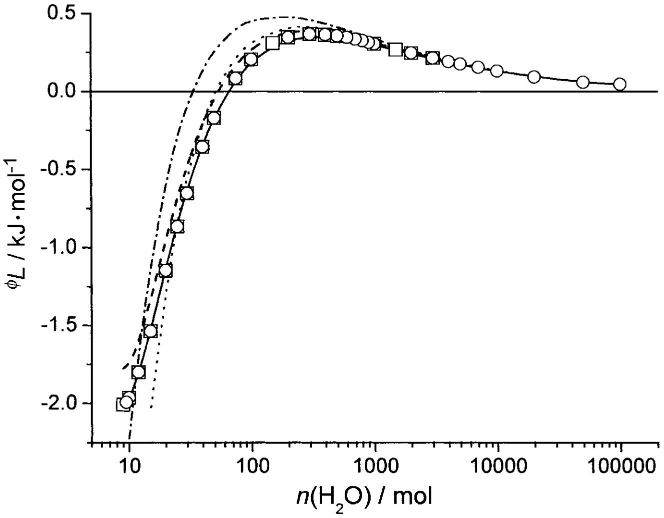

Fig. 2. Apparent molar relative enthalpy of NaCl(aq) at 25°C; experimental data: circles [58], squares [59]; calculated values: solid line, present model; dashed line [31]; dotted line, SIT model with lower weight on data at high molalities; dash-dot line, SIT model with equal weights on all data

is inferior to the more flexible, 3-parameter *Pitzer* model. In any case, the SIT model seems less suitable for representing these data to saturation molalities.

The present constant heat capacity *Pitzer* model satisfactorily reproduces enthalpies of solution of NaCl(s) measured recently between 25°C and 60°C [68] (Fig. 3). However, when the present model is used to extrapolate relative apparent

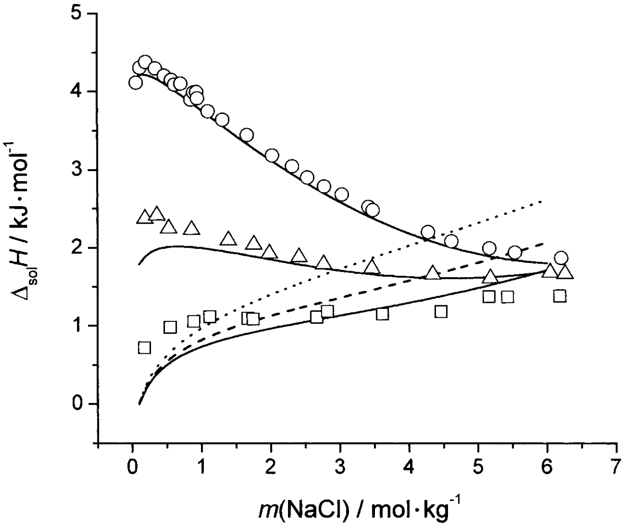

Fig. 3. Enthalpies of dissolution of NaCl(*s*) at 24.4°C (circles), 44.3°C (triangles), and 59.2°C (squares) [68]; calculated values: solid lines, present model at these temperatures; dashed line, according to Eq. (21) at 59.2°C; dotted line, according to Eq. (20) at 59.2°C

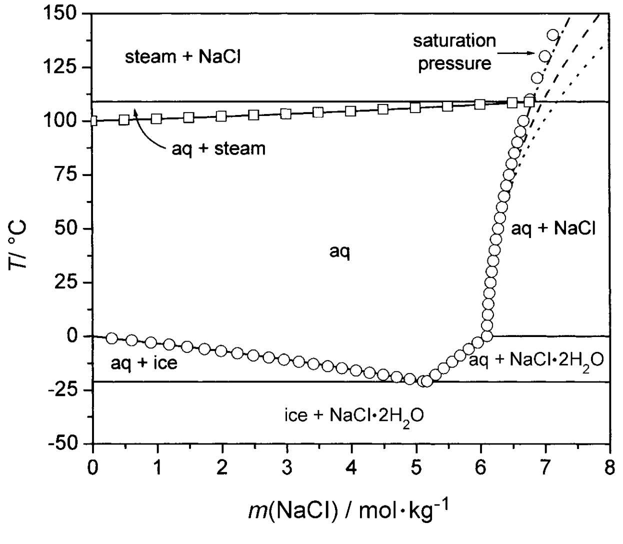

Fig. 4. Temperature-composition phase diagram of the NaCl–H_2O system at $P = 1.01325$ bar and at saturation pressure; experimental data: circles [70]; boiling points: squares, as tabulated by *Clarke* and *Glew* [57]; calculated values: solid and dash-dot lines, present model; dashed line, according to Eq. (21); dotted line, according to Eq. (20)

molar enthalpies to 100°C, deviations of about 20% from the values of Ref. [32] are noted. Similar deviations have been obtained by *Gates et al.* [69], although these authors used a more refined, temperature dependent heat capacity model based on their highly precise measurements.

Figure 4 shows the temperature-composition phase diagram of the NaCl–H_2O system. The present model reproduces experimental data for all equilibria between

Table 3. Ternary and neutral-species interaction parameters; the temperature independent values have been reported for 25°C

i	j	k	${}^{S}\theta_{ij}$	ψ_{ijk}	λ_{ij}
H^+	Na^+	Cl^-	0.036[a]	−0.004[a]	
Cl^-	OH^-	Na^+	−0.05[a]	−0.006[a]	
				$-9.93(T/K)^{-1}+0.0273$[b]	
Cl^-	HCO_3^-	Na^+	0.0359[c]	−0.0143[c]	
Cl^-	CO_3^{2-}	Na^+	−0.053[c]	0.016[d]	
				$11.18(T/K)^{-1}-0.0235$[e]	
$CO_2(aq)$	Na^+				0.10[f]
$CO_2(aq)$	Cl^-				−0.005[f]

[a] *Pitzer* and *Kim* [74]; [b] *Pabalan* and *Pitzer* [6], see text; [c] *Peiper* and *Pitzer* [51]; [d] *Thurmond* and *Millero* [75]; [e] this study, see text; [f] *Harvie et al.* [4]

−21 and 110°C very well; even up to 150°C the agreement with solubility data [70] is quite reasonable. The two other extrapolation methods, Eq. (21) and particularly Eq. (20), which do not correspond to constant heat capacities, result in significant deviations above about 85 and 65°C respectively.

An independent test of the present model is provided by the prediction of equilibrium constants in a mixed electrolyte solution. The ionic product of water, defined by $K_w = m(H^+)m(OH^-)$, has been precisely measured in NaCl(aq) by hydrogen electrode potentiometry in the temperature range from 25 to 300°C [71–73]. In these studies, the NaCl solution must actually be regarded as a four-component system (HCl–NaOH–NaCl–H_2O). In addition to the NaCl parameters, the binary *Pitzer* parameters for NaOH (see below) and HCl [2, 31, 47, 49] were extrapolated to high temperatures according to the present method (Eq. (22)). Also, four ternary mixing parameters valid at 25°C have been reported [74] (see Table 3) which were extrapolated according to Eq. (23). Most surprisingly, $\log K_w$ values calculated from the present model agree with measured values within the experimental uncertainties up to at least 250°C (Figs. 5 and 6). Presumably, there is some sort of error compensation involved at high temperatures, but the better predictive power of the present method (Eqs. (22) and (23)) compared to Eq. (20) is nonetheless obvious.

Sodium Carbonate, Hydrogen Carbonate, and Hydroxide

Vanderzee [80] and *Peiper* and *Pitzer* [51] have thoroughly analyzed the thermodynamic properties of aqueous solutions of sodium carbonate and its hydrolysis products hydrogen carbonate and hydroxide. In the early 1980's, when their work was done, experimental data were only available at 25°C. Very recently, *Polya et al.* (Oak Ridge National Laboratory) [45] have measured the enthalpies of dilution of $Na_2CO_3(aq)$ and $NaHCO_3(aq)$ at moderate molalities (up to $m = 1.5\,\mathrm{mol \cdot kg^{-1}}$) from $T = 25$ to 250°C and at pressures of $P = 70$ and 400 bar. To correlate their data, *Polya et al.* [45] employed a comprehensive *Pitzer* model with *Peiper* and *Pitzer*'s [51] parameters for 25°C and 13 enthalpy parameters for each pressure.

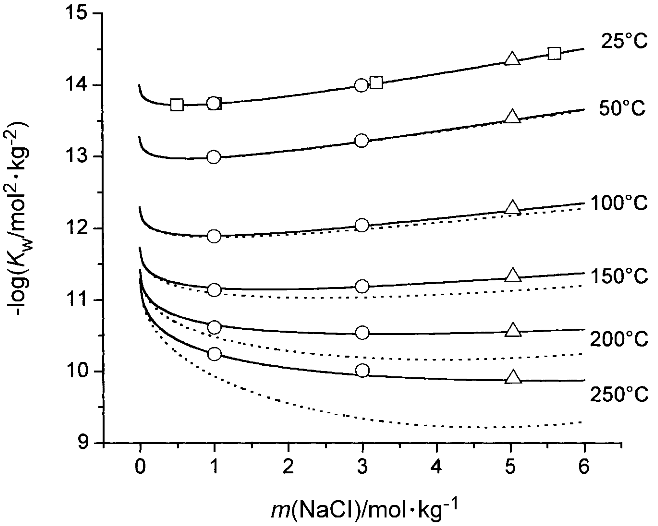

Fig. 5. Ionic product of water in NaCl(*aq*); experimental data: squares [71]; circles [72], triangles [73]; calculated values: solid lines, present model; dotted lines, according to Eq. (20)

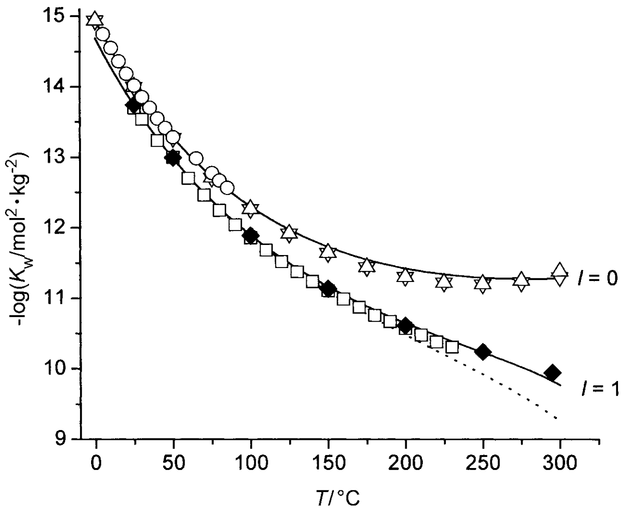

Fig. 6. Ionic product of water at $I = 0$ and $I = 1\,\mathrm{mol \cdot kg^{-1}}$ NaCl as a function of temperature; experimental values: diamonds [72], squares [76], circles [77], up-triangles [78], down-triangles [79]; calculated values: solid lines, present model; dotted line, according to Eq. (20)

Peiper and *Pitzer* [51] used the *Pitzer* model to derive binary interaction parameters together with their temperature dependencies and parameters for ternary interactions among the mentioned ions and with chloride. In view of the geochemical importance, *Monnin* and *Schott* [5] developed a model to calculate the solubilities of sodium carbonate minerals in brines. These authors employed *Peiper* and *Pitzer*'s aqueous model together with additional parameters taken from *Harvie et al.* [4] to derive standard enthalpies of formation and standard entropies of the solid phases from solubility data. Using these quantities together with *Peiper* and

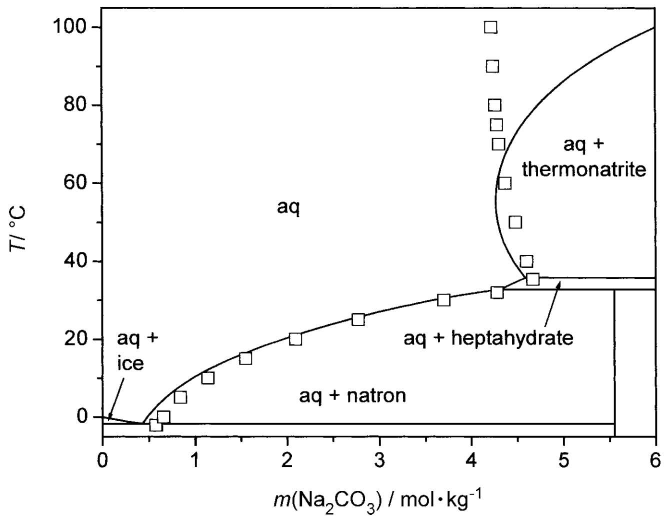

Fig. 7. Phase diagram of the Na_2CO_3–H_2O system; experimental data are from Ref. [81]; calculated values were obtained using data from Ref. [5]

Pitzer's temperature dependent interaction parameters according to Eq. (20) results in the Na_2CO_3–H_2O phase diagram shown in Fig. 7. Due to the poor agreement with experimental solubility data and the fact noticed earlier [19, 20] that *Monnin* and *Schott*'s quantities for the solid phases disagree with values carefully derived from calorimetric data [63, 82], a new assessment of this heterogeneous system seemed worthwhile.

As for NaCl, the present model uses the classical *Pitzer* equations with the parameters given in Table 1. The parameters valid at 25°C for Na_2CO_3 and $NaHCO_3$ were taken from *Peiper* and *Pitzer* [51], those for NaOH from *Pitzer* and *Mayorga* [47]. Enthalpy and heat capacity parameters for $NaHCO_3$ [51] were found satisfactory. For NaOH, the heat capacity parameters were taken from *Criss* and *Millero* [49], and the enthalpy parameters were re-determined to give a better fit to the data from Refs. [35, 58] at higher molalities (Fig. 8). Although the SIT model was appropriate to represent solubilities of sparingly soluble electrolytes in $NaClO_4$ media [18], it is obviously not suitable for representing apparent molar relative enthalpies of NaOH(*aq*) at higher molalities. The Na_2CO_3 enthalpy parameters reported by *Peiper* and *Pitzer* [51] reproduce experimental values only at low molalities, which is not surprising as these authors used only two parameters. Therefore, three parameters were fitted to the apparent molar relative enthalpies of Na_2CO_3 at 25°C given in Table 3 of Ref. [83], which are essentially the same as those reported in the NBS tables [59]. For the same reason as in the case of NaCl, a higher weight was given to the data points closest to saturation. To model the apparent molar heat capacities of Na_2CO_3, the $\beta^{(0)J}$ and $\beta^{(1)J}$ parameters given by *Peiper* and *Pitzer* [51] were retained. These parameters were derived from measurements performed up to 1 mol · kg^{-1} [84]. In addition, a C^J parameter was estimated in order to reproduce data at higher molalities measured by *Chernen'kaya* [85] (Fig. 9).

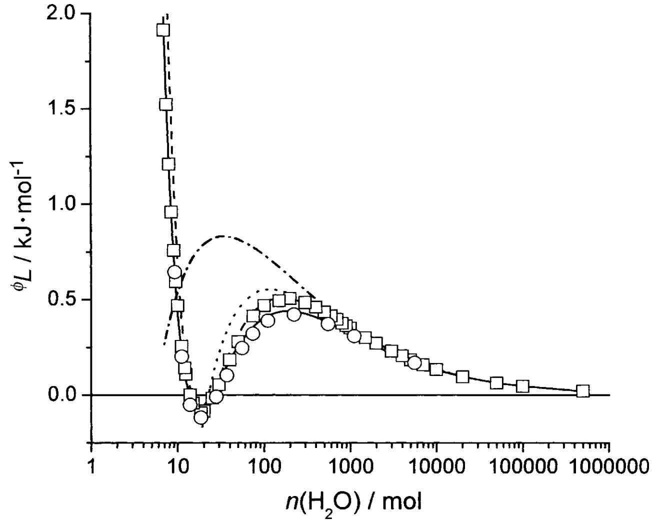

Fig. 8. Apparent molar relative enthalpy of NaOH(aq) at 25°C; experimental data: circles [35], squares [58]; calculated values: solid line, present model; dashed line [31]; dotted line, SIT model with lower weight on data at high molalities; dash-dot line, SIT model with equal weights on all data

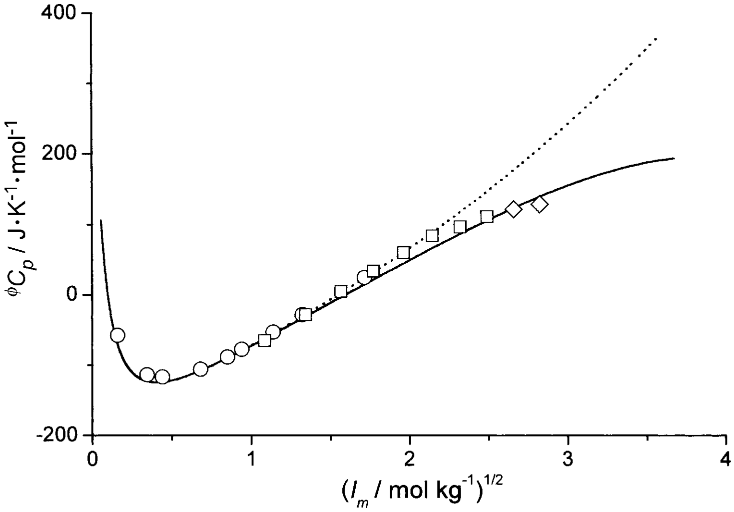

Fig. 9. Apparent molar heat capacity of Na_2CO_3(aq) at 25°C; experimental data: circles [84]; squares [85]; diamonds [86]; calculated values: solid line, present model; dotted line [51]

It should be noted that equilibrium enthalpy and heat capacity data were used in these optimizations. Owing to hydrolysis, hydrogen carbonate and hydroxide ions are formed at equilibrium. Since the degree of hydrolysis increases with dilution, the contribution of the enthalpy of hydrolysis becomes larger at low molalities as can be seen from Fig. 10. The effect of temperature on the chemical equilibria leads to a so-called 'relaxation' contribution to the measured heat capacity of the solution which results in an increase of $^{\phi}C_p$ at low ionic strengths (Fig. 9) as has been discussed *e.g.* by *Peiper* and *Pitzer* [51] and *Vanderzee* [80]. *Hepler* and

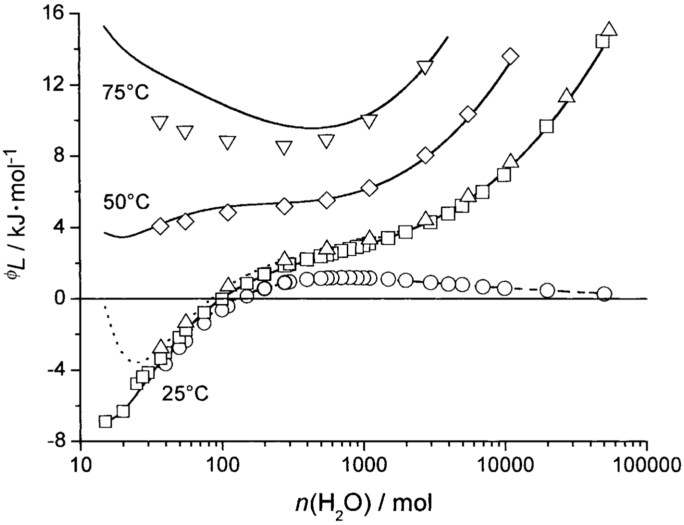

Fig. 10. Apparent molar relative enthalpies of $Na_2CO_3(aq)$; experimental data at 25°C: squares [59, 83], up-triangles [45]; circles, data corrected with respect to hydrolysis [83]; at 50°C: diamonds [45]; at 75°C: down-triangles [45]; calculated values: solid lines, present model; dashed line, present model, hydrolysis suppressed; dotted line, enthalpy parameters from Ref. [45]

Hovey [87] show that the relaxation contribution is always positive and give many references to systems for which this effect has been observed. However, an analytical expression of the relaxation contribution is different for nearly every system that has been investigated and sometimes quite cumbersome to derive.

In ChemSage, heat capacities and enthalpies are calculated by appropriate numerical differentiation of equilibrium *Gibbs* energies with respect to temperature. In this way, chemical reactions and shifts of equilibria with temperature, and thus the effects mentioned above, are automatically accounted for. If one wants to calculate the properties of hypothetical, pure electrolytes, the effects of equilibria and relaxation can easily be suppressed by disregarding the reaction products in the calculation. Therefore, ChemSage or F*A*C*T are truly 'facilities for the analysis of chemical thermodynamics' that allow the user to deal with these effects correctly without the need of performing complicated thermodynamic derivations.

The standard enthalpies of formation and standard entropies of sodium carbonate decahydrate (natron), heptahydrate, and monohydrate (thermonatrite) were optimized with respect to solubility data. The *Bayes* formalism [88, 89] used in the ChemSage optimizer [15] permits to weight parameters (in this case, the standard thermodynamic quantities of the solids) and experimental data (solubilities) independently from each other. Thereby, the carefully evaluated calorimetric quantities reported by *Vanderzee* [63, 82] were used as *a priori* parameters and their weights were chosen such that they changed essentially within their reported uncertainties. With an ordinary least-squares optimization, the changes in the parameter values would be much larger.

The phase diagram thus calculated agrees very reasonably with experimental data given by *Linke* and *Seidell* [81] (Fig. 11). Also, heptahydrate and thermonatrite solubilities are well reproduced in the metastable range, although these data

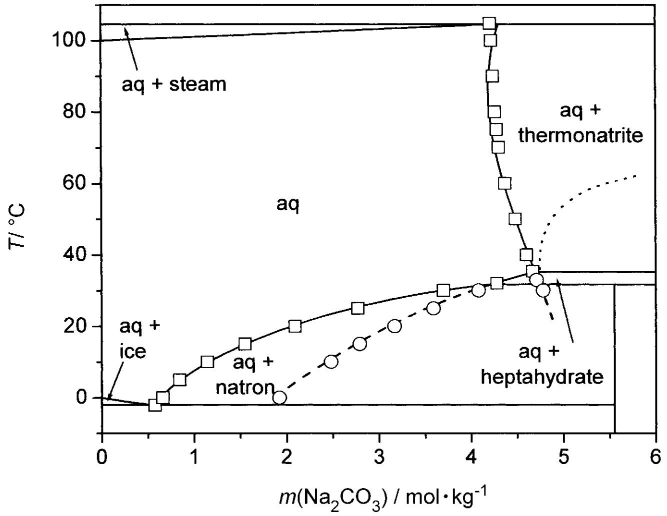

Fig. 11. Phase diagram of the Na_2CO_3–H_2O system; experimental data: squares, stable equilibria; circles, metastable equilibria [81]; calculated curves according to the present model: solid lines, stable equilibria; dashed lines, metastable equilibria; dotted line: thermonatrite solubility calculated from the present model but with $C^J = 0$, *i.e.* with *Peiper* and *Pitzer*'s [51] heat capacity parameters only

were not used in the optimizations. Figure 11 also illustrates the importance of correct apparent molar heat capacity values close to saturation. Obviously, *Peiper* and *Pitzer*'s [51] model ($C^J = 0$), which wrongly extrapolates to high molalities (dotted line in Fig. 9), results in a completely wrong solubility prediction (dotted line in Fig. 11). It should also be noted that C^J and the standard thermodynamic quantities of thermonatrite are strongly correlated and it is quite difficult to determine optimal values. This explains that the change in the *a priori* parameters for thermonatrite had to be larger than the experimental uncertainties in order to reproduce experimental solubilities. However, there is still some discrepancy at temperatures above 90°C where calculated solubilities start to increase again.

The present model was also used to predict relative apparent molar enthalpies of $Na_2CO_3(aq)$ at higher temperatures (Fig. 10). Whereas the agreement with the data measured by *Polya et al.* [45] is nearly perfect at 50°C, it becomes worse at 75°C, similar to the findings for NaCl. Unfortunately, *Polya et al.* limited their measurements to $m = 1.5\,\mathrm{mol \cdot kg^{-1}}$, whereas solubilities of thermonatrite range beyond $4\,\mathrm{mol \cdot kg^{-1}}$. Almost inevitable with the *Pitzer* model, extrapolations of enthalpies and heat capacities to higher molalities are rather poor. Particularly, using the enthalpy parameters of Ref. [45] for 25°C, the partial molar enthalpy of $Na_2CO_3(aq)$ changes its sign close to saturation, thus leading to a strong increase rather than to the slight decrease observed experimentally for thermonatrite solubilities just above 40°C. It must be concluded that despite the high quality of the ORNL data, the *Pitzer* model based on them fails completely to predict sodium carbonate solubilities. As has been noted by *Peiper* and *Pitzer* [51] two decades ago, measurements of heat capacities and enthalpies of dilution up to saturation are very desirable; however, they are still lacking for this important system.

Solubility Predictions for Multicomponent Electrolyte Systems

The data obtained in this work were used to predict solubilities in the ternary systems Na_2CO_3–$NaCl$–H_2O and Na_2CO_3–$NaOH$–H_2O and in the quaternary system Na_2CO_3–$NaCl$–$NaOH$–H_2O for $0°C \leq T \leq 100°C$.

The NaCl–NaOH–H_2O system

Pabalan and *Pitzer* [6] considered it necessary to introduce a temperature dependent ternary interaction parameter $\psi_{Na,OH,Cl} = -9.93(T/K)^{-1} + 0.0273$ (which results in $\psi_{Na,OH,Cl} = -0.006$ for 25°C [74]) in order to reproduce NaCl solubilities in NaOH solutions at temperatures different from 25°C. If their $\psi_{Na,OH,Cl}$ is used with the present model, the results between 0 and 100°C are of similar quality as in *Pabalan* and *Pitzer*'s work [6]. This temperature dependent $\psi_{Na,OH,Cl}$ parameter also influences pK_w values calculated at higher temperatures (see Fig. 5). The results obtained are slightly worse than with the temperature independent $\psi_{Na,OH,Cl}$ parameter [74] but still in very good agreement with experimental values.

The Na_2CO_3–NaOH–H_2O system

Solubilities are in general well reproduced, particularly at higher temperatures (Fig. 12). At low temperatures (Fig. 13), the natron solubilities agree very well with experimental data, whereas measured solubilities of heptahydrate and thermonatrite are generally higher than the calculated values. This may be either due to experimental difficulties (*e.g.* supersaturation) or model imperfections (*e.g.* wrong extrapolation of the *Gibbs* energies of these phases to low temperatures). However, metastable solubilities in water are very well modelled (Fig. 11), and changing ternary parameters would also affect natron solubilities. Thus, it is suggested that more solubility data are measured for this system at low temperatures.

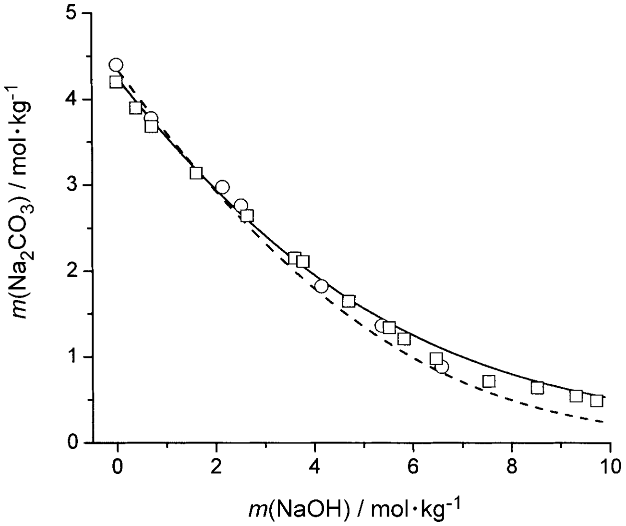

Fig. 12. Solubility of thermonatrite in NaOH solutions as calculated from the present model; experimental data were taken from Ref. [81]; circles, dashed line, 60°C; squares, solid line, 100°C

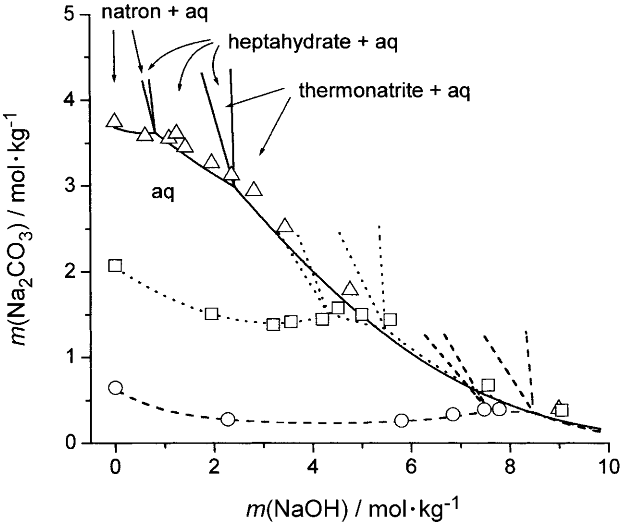

Fig. 13. Isothermal phase diagrams of the Na_2CO_3–NaOH–H_2O system; experimental data from Ref. [81]: circles, 0°C; squares, 20°C; triangles, 30°C; calculated values from the present model: the curves for the corresponding temperatures are dashed, dotted, and solid, respectively; one-, two-, and three-phase fields are indicated at the 30°C phase diagram

It should be noted that these phase diagrams, which have been conveniently generated using the so-called two-dimensional phase mapping feature of ChemSage, are of Type III in *Pelton* and *Schmalzried*'s [90, 91] classification. This means that two molar quantities are plotted against each other, whereas thermodynamic potentials like temperature and pressure are kept constant. In this type of phase diagrams, one-, two-, and three-phase fields are all two-dimensional. In the literature, however, usually only the solubility curves are depicted, whereas the other phase fields are omitted.

The Na_2CO_3–NaCl–H_2O system

Solubilities calculated with the temperature independent ternary parameters given in Table 3 are already reasonable, although they are a bit lower than experimental values, especially at higher temperatures. If, similar to NaCl–NaOH–H_2O, a temperature dependent parameter $\psi_{\mathrm{Na,CO_3,Cl}} = 11.18(T/\mathrm{K})^{-1} - 0.0235$, which essentially retains the 25°C value, is introduced, the agreement with experimental data can be improved (Figs. 14 and 15). Surprisingly, there is a lack of solubility data for this important system, so that the measurement of new solubility data is strongly recommended, particularly for temperatures above 25°C.

The Na_2CO_3–NaCl–NaOH–H_2O system

Phase diagrams for this system at NaCl saturation agree reasonably well with experimental data [81], despite the high ionic strengths of these mixed electrolyte solutions (Fig. 16). No further parameters have been adjusted; the results can therefore be regarded as a true prediction of solubilities in a multicomponent

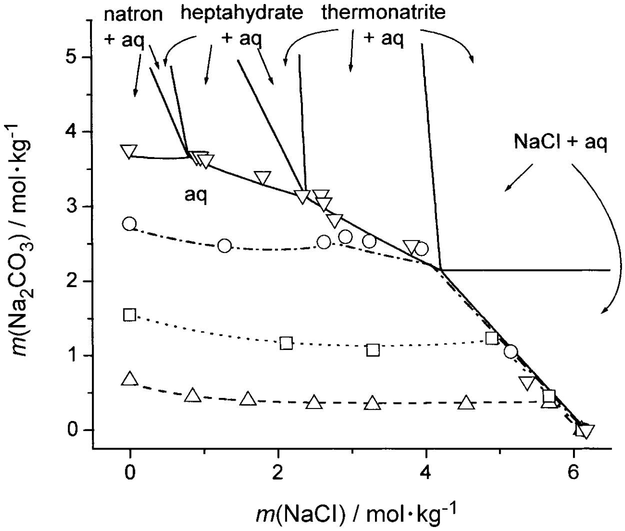

Fig. 14. Isothermal phase diagrams of the Na_2CO_3–NaCl–H_2O system; experimental data from Ref. [81]: up-triangles, 0°C; squares, 15°C; circles, 25°C; down-triangles, 30°C; calculated values from the present model: the curves for the corresponding temperatures are dashed, dotted, dash-dot, and solid, respectively; one-, two-, and three-phase fields are indicated at the 30°C phase diagram

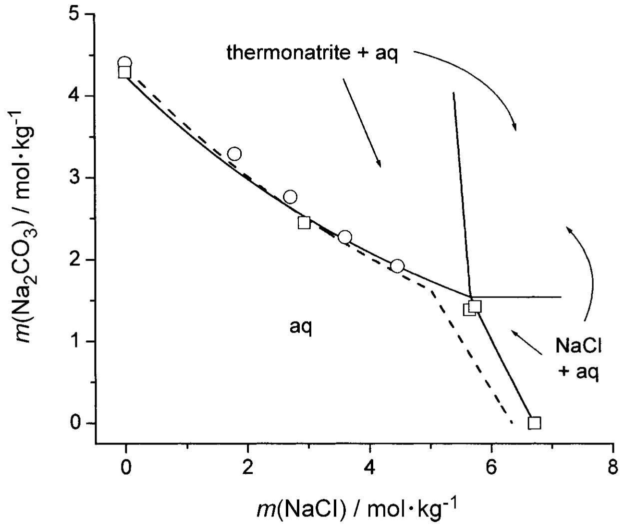

Fig. 15. Isothermal phase diagrams of the Na_2CO_3–NaCl–H_2O system as calculated from the present model; experimental data were taken from Ref. [81]; circles, dashed line, 60°C; squares, solid line, 100°C

electrolyte system. However, there are some discrepancies that can be analyzed by investigating the effects of changing thermodynamic data on calculated solubilities. For instance, whereas thermonatrite solubilities agree perfectly with experimental data at 60°C, making this phase less stable by about 600 J · mol^{-1} would result in very good agreement at lower temperatures. However, this change in the standard *Gibbs* energy is not compatible with solubilities in pure water. At higher

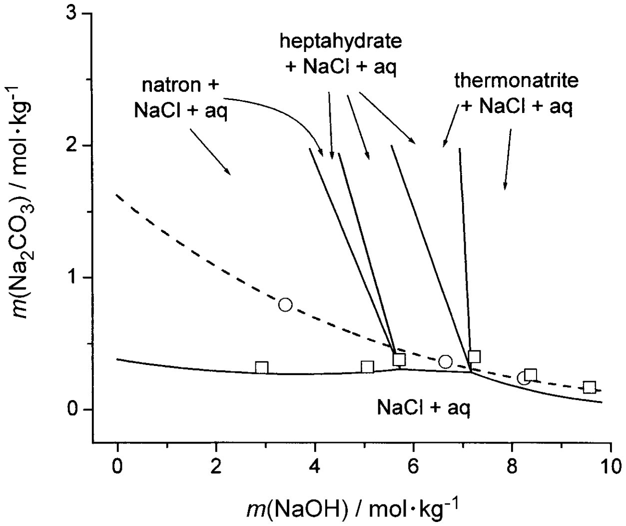

Fig. 16. Isothermal phase diagrams of the $Na_2CO_3-NaCl-NaOH-H_2O$ system at NaCl saturation as calculated from the present model; experimental data are from Ref. [81]; circles, dashed line, 60°C; squares, solid lines, 0°C

temperatures, assigning a value to ψ_{Na,OH,CO_3} (which was not needed for the Na_2CO_3–NaOH–H_2O subsystem) may be more appropriate. This obviously points at the limitations of the present method with its temperature independent heat capacities for aqueous and solid phases. Using the flexibility of the *Pitzer* model, a full optimization of the system could be performed (*i.e.* by taking all available experimental information into account). This would lead to complicated temperature functions of standard *Gibbs* energies and *Pitzer* parameters which is, however, beyond the scope of this study.

Discussion and Conclusions

Although *Pitzer* models are constantly improved for a limited number of electrolytes, there is a need for simple models which can use the little information that is available for the vast majority of electrolytes. It has been shown that *Pitzer* parameters for the osmotic coefficient, apparent molar relative enthalpy, and heat capacity, all valid for 25°C, can be employed to predict solubilities in the temperature range from 0 to 100°C. It is most important, however, that the parameters are (*i*) adjusted to data measured up to saturation and then (*ii*) properly extrapolated to higher temperatures. Of the three methods examined here, Eqs. (22) and (23) proposed in this work were found most satisfactory. This new method corresponds to constant heat capacities of the solution, apart from the temperature dependence of the *Debye-Hückel* coefficient A_J. Previously, constant standard heat capacities of reaction have been found appropriate to reproduce standard equilibrium constants very accurately in the temperature range from 0 to 100°C or even higher [19, 92]. Also, the so-called density model, in its modification by *Anderson et al.* [93], is essentially a constant heat capacity model at these temperatures.

Solubility predictions for complex systems are quite reasonable when temperature independent ternary *Pitzer* parameters are used, but they can certainly be improved when some temperature dependence of the ψ parameters is introduced. As the latter is usually fitted to solubility data [6], one must be careful not to use the same data for parametrization and then for proving the predictive capabilities of the model. In general, solubilities in complex media can be used to validate models, as calculated solubility values are very sensitive to changes in the ternary interaction parameters.

Lu et al. [94, 95] have recently proposed a *semi*-empirical model that uses ion-specific parameters and a universal relation for the influence of temperature on some model parameters which is obtained by a least squares fit to experimental activity and osmotic coefficients of 13 electrolytes between 50 and 300°C. Also, four temperature coefficients for each solubility product have been fitted to salt solubilities in water. These authors claim that their model can predict osmotic and activity coefficients, apparent molar enthalpies, and solubilities (the latter in mixed electrolyte solutions) over wide ranges of temperatures. In the present communication, the word 'prediction' has a different meaning, as no fitting to properties as a function of temperature is involved.

The ChemSage software used in this work is a true facility for the analysis of chemical thermodynamics. It is capable of calculating solubilities in complex media, integral and partial thermodynamic quantities of phases, and complete phase diagrams quickly and conveniently. This software is also invaluable for studying the interrelations and correlations among the various interaction parameters, thermodynamic quantities of solids, and experimental data. Thereby, different scenarios can be designed that help to identify the conditions for which new solubility measurements should be performed. Such suggestions have particularly been made regarding the measurement of sodium carbonate solubilities in various salt solutions. For this task, a recently developed solubility apparatus by *Capewell et al.* [96] could be favourably used.

The results of the present work make it seem feasible that the currently available information on *Pitzer* parameters at 25°C can be employed to establish databases for solubility predictions in complex systems from 0°C to 100°C.

Acknowledgements

I am grateful to Profs. *Peter May* and *Glenn Hefter* (Murdoch University, Western Australia) for stimulating discussions on solution chemistry and thermodynamic modelling. Prof. *May* also pointed out the significance of the density model to the present work.

References

[1] Primas H (1983) Chemistry, Quantum Mechanics and Reductionism, 2nd edn. Springer, Berlin
[2] Pitzer KS (1991) In: Pitzer KS (ed) Activity Coefficients in Electrolyte Solutions, 2nd edn. CRC Press, Boca Raton, p 75
[3] Harvie CE, Weare JH (1980) Geochim Cosmochim Acta **44**: 981
[4] Harvie CE, Møller N, Weare JH (1984) Geochim Cosmochim Acta **48**: 723
[5] Monnin C, Schott J (1984) Geochim Cosmochim Acta **48**: 571
[6] Pabalan RT, Pitzer KS (1987) Geochim Cosmochim Acta **51**: 2429

[7] Pabalan RT, Pitzer KS (1991) In: Pitzer KS (ed) Activity Coefficients in Electrolyte Solutions, 2nd edn. CRC Press, Boca Raton, p 435

[8] Møller N (1988) Geochim Cosmochim Acta **52**: 821

[9] Greenberg JP, Møller N (1989) Geochim Cosmochim Acta **53**: 2503

[10] Spencer RJ, Møller N, Weare JH (1990) Geochim Cosmochim Acta **54**: 575

[11] Monnin C (1995) J Chem Eng Data **40**: 828

[12] Monnin C (1999) Chem Geol **153**: 187

[13] Marion GM, Farren RE (1999) Geochim Cosmochim Acta **63**: 1305

[14] Kaufman L, Bernstein H (1970) Computer Calculation of Phase Diagrams. Academic Press, New York

[15] Königsberger E, Eriksson G (1995) CALPHAD **19**: 207

[16] Gamsjäger H, Königsberger E, Preis W (1998) Pure Appl Chem **70**: 1913

[17] Gamsjäger H, Preis W, Königsberger E, Magalhaes MCF, Brandao P (1999) J Solution Chem **28**: 711

[18] Preis W, Königsberger E, Gamsjäger H (2000) J Solution Chem **29**: 605

[19] Königsberger E, Königsberger L-C, Gamsjäger H (1999) Geochim Cosmochim Acta **63**: 3105

[20] Königsberger E, Königsberger L-C, Gamsjäger H (2001) Geochim Cosmochim Acta **65**: 183

[21] Königsberger E, Gamsjäger H (1987) Ber Bunsenges Phys Chem **91**: 785

[22] Königsberger E, Schmidt P, Gamsjäger H (1992) J Solution Chem **21**: 1195

[23] Nguyen AM, Königsberger E, Marhold H, Gamsjäger H (1993) Monatsh Chem **124**: 1011

[24] Gamsjäger H, Marhold H, Königsberger E, Tsai YJ, Kolmer H (1995) Z Naturforsch **50a**: 59

[25] Königsberger E, Tran-Ho L-C, Gamsjäger H (1998) Monatsh Chem **129**: 1061

[26] Gamsjäger H, Königsberger E, Preis W (2000) Aquatic Geochem **6**: 119

[27] Königsberger E, Eriksson G (1999) J Solution Chem **28**: 721

[28] Grenthe I, Plyasunov AV, Spahiu K (1997) In: Grenthe I, Puigdomenech I (eds) Modelling in Aquatic Chemistry, Nuclear Energy Agency. OECD, Paris, p 325

[29] Pitzer KS (1973) J Phys Chem **77**: 268

[30] Mesmer RE, Palmer DA, Simonson JM, Holmes HF, Ho PC, Wesolowski DJ, Gruszkiewicz MS (1997) Pure Appl Chem **69**: 905

[31] Silvester LF, Pitzer KS (1978) J Solution Chem **7**: 327

[32] Busey RH, Holmes HF, Mesmer RE (1984) J Chem Thermodyn **16**: 343

[33] Holmes HF, Mesmer RE (1986) J Chem Thermodyn **18**: 263

[34] Hovey JK, Pitzer KS, Rard JA (1993) J Chem Thermodyn **25**: 173

[35] Simonson JM, Mesmer RE, Rogers PSZ (1989) J Chem Thermodyn **21**: 561

[36] Holmes HF, Busey RH, Simonson JM, Mesmer RE, Archer DG, Wood RH (1987) J Chem Thermodyn **19**: 863

[37] Ananthaswamy J, Atkinson G (1985) J Chem Eng Data **30**: 120

[38] Archer DG (1991) J Phys Chem Ref Data **20**: 509

[39] Archer DG (1992) J Phys Chem Ref Data **21**: 793

[40] Clegg SL, Rard JA, Pitzer KS (1994) J Chem Soc Faraday Trans **90**: 1875

[41] Pitzer KS, Wang P, Rard JA, Clegg SL (1999) J Solution Chem **28**: 265

[42] Silvester LF, Pitzer KS (1977) J Phys Chem **81**: 1822

[43] Bradley DJ, Pitzer KS (1979) J Phys Chem **83**: 1599

[44] Archer DG, Wang P (1990) J Phys Chem Ref Data **19**: 371

[45] Polya DA, Woolley EM, Simonson JM, Mesmer RE (2001) J Chem Thermodyn **33**: 205

[46] Pitzer KS, Peiper JC, Busey RH (1984) J Phys Chem Ref Data **13**: 1

[47] Pitzer KS, Mayorga G (1973) J Phys Chem **77**: 2300

[48] Pitzer KS, Mayorga G (1974) J Solution Chem **3**: 539

[49] Criss CM, Millero FJ (1996) J Phys Chem **100**: 1288

[50] Criss CM, Millero FJ (1999) J Solution Chem **28**: 849

[51] Peiper JC, Pitzer KS (1982) J Chem Thermodyn **14**: 613

[52] Roy RN, Gibbons JJ, Williams R, Godwin L, Baker G, Simonson JM, Pitzer KS (1984) J Chem Thermodyn **16**: 303

[53] Bale CW, Pelton AD (1999) FACT-Win – User Manual. CRCT, Ecole Polytechnique de Montréal, Québec, Canada (http://www.crct.polymtl.ca)

[54] Pelton AD (2000) personal communication

[55] Eriksson G, Hack K (1990) Metall Trans **21B**: 1013

[56] Helgeson HC, Kirkham DH, Flowers GC (1981) Am J Sci **281**: 1249

[57] Clarke ECW, Glew DN (1985) J Phys Chem Ref Data **14**: 489

[58] Parker VB (1965) Thermal Properties of Aqueous Uni-univalent Electrolytes, US Nat Bur Standards, NSRDS-NBS 2

[59] Wagman DD, Evans WH, Parker VB, Schumm RH, Halow I, Bailey SM, Churney KL, Nuttall RL (1982) J Phys Chem Ref Data **11** (Supplement 2)

[60] Williamson AT (1944) Trans Faraday Soc **40**: 421

[61] Cox JD, Wagman DD, Medvedev VA (1989) CODATA Key Values for Thermodynamics. Hemisphere Publishing, New York

[62] Archer DG (1997) J Chem Eng Data **42**: 281

[63] Vanderzee CE (1982) J Chem Thermodyn **14**: 219

[64] Tsonopoulos C (1974) AIChE J **20**: 273

[65] Tanner JE, Lamb FW (1978) J Solution Chem **7**: 303

[66] Perron G, Roux AH, Desnoyers JE (1981) Can J Chem **59**: 3049

[67] Saluja PPS, Jobe DJ, LeBlanc JC, Lemire RJ (1995) J Chem Eng Data **40**: 398

[68] Hubert N, Solimando R, Pere A, Schuffenecker L (1997) Thermochim Acta **294**: 157

[69] Gates JA, Tillett DM, White DE, Wood RH (1987) J Chem Thermodyn **19**: 131

[70] Cohen-Adad R, Lorimer JW (1991) Alkali Metal and Ammonium Halides in Water and Heavy Water (Binary Systems), IUPAC Solubility Data Series, vol 47. Pergamon Press

[71] Kron I, Marshall SL, May PM, Hefter G, Königsberger E (1995) Monatsh Chem **126**: 819

[72] Busey RH, Mesmer RE (1976) J Solution Chem **5**: 147

[73] Palmer DA, Drummond SE (1988) J Solution Chem **17**: 153

[74] Pitzer KS, Kim JJ (1974) J Am Chem Soc **96**: 5701

[75] Thurmond V, Millero FJ (1982) J Solution Chem **11**: 447

[76] Becker P, Bilal BA (1985) J Solution Chem **14**: 367

[77] Bezboruah CP, Filomen J, Camoes GFC, Covington AK, Dobson JV (1973) J Chem Soc Faraday Trans 1 **69**: 949

[78] Chen X, Oscarson JL, Gillespie SE, Cao H, Izatt RM (1994) J Solution Chem **23**: 747

[79] Sweeton FH, Mesmer RE, Baes CF Jr (1974) J Solution Chem **3**: 191

[80] Vanderzee CE (1982) J Chem Thermodyn **14**: 1051

[81] Linke WF and Seidell A (1965) Solubilities. Inorganic and Metal-Organic Compounds, vol 2. American Chemical Society

[82] Berg RL, Vanderzee CE (1978) J Chem Thermodyn **10**: 1113

[83] Berg RL, Vanderzee CE (1978) J Chem Thermodyn **10**: 1049

[84] Perron G, Desnoyers JE, Millero FJ (1975) Can J Chem **53**: 1134

[85] Chernen'kaya EI (1971) Zh Prikl Khim **44**: 1543

[86] Aseyev GG (1996) Thermal Properties of Electrolyte Solutions. Begell House, New York

[87] Hepler LG, Hovey JK (1996) Can J Chem **74**: 639

[88] Königsberger E, Gamsjäger H (1990) Monatsh Chem **121**: 119

[89] Königsberger E (1991) CALPHAD **15**: 73

[90] Pelton AD, Schmalzried H (1973) Met Trans **4**: 1395

[91] Königsberger E, Gamsjäger H (1991) Ber Bunsenges Phys Chem **95**: 734

[92] Puigdomenech I, Rard JA, Plyasunov AV, Grenthe I (1997) In: Grenthe I, Puigdomenech I (eds) Modelling in Aquatic Chemistry. Nuclear Energy Agency, OECD, Paris, p 427
[93] Anderson GM, Castet S, Schott J, Mesmer RE (1991) Geochim Cosmochim Acta **55**: 1769
[94] Lu X, Zhang L, Wang Y, Shi J, Maurer G (1996) Ind Eng Chem Res **35**: 1777
[95] Lu X, Zhang L, Wang Y, Shi J (1996) Fluid Phase Equil **116**: 201
[96] Capewell SG, Hefter GT, May PM (1999) Rev Sci Instrum **70**: 1481

Received April 20, 2001. Accepted May 2, 2001